NATIONAL ADVISORY COMMITTEE FOR AERONAUTICS

# WARTIME REPORT

ORIGINALLY ISSUED

August 1945 as
Advance Restricted Report L5F25a

## STABILITY AND CONTROL CHARACTERISTICS OF A FIGHTER AIRPLANE IN INVERTED FLIGHT ATTITUDE AS DETERMINED BY MODEL TESTS

By John W. Paulson and Charles V. Bennett

Langley Memorial Aeronautical Laboratory
Langley Field, Va.




WASHINGTON

NATIONAL ADVISORY COMMITTEE FOR AERONAUTICS

ADVANCE RESTRICTED REPORT

# STABILITY AND CONTROL CHARACTERISTICS OF A FIGHTER AIRPLANE IN INVERTED FLIGHT ATTITUDE AS DETERMINED BY MODEL TESTS

By John W. Paulson and Charles V. Bennett

## SUMMARY

Tests have been made in the Langley free-flight tunnel to compare the stability and control characteristics of a powered airplane model in the erect and in the inverted flight attitudes. Force tests and yaw-trim tests were made to determine the static stability characteristics of the model and power-off flight tests were made to determine the general flight characteristics of the model in the inverted attitude.

The results of the tests showed that with zero thrust the longitudinal and directional stability was almost the same in the inverted flight attitude as in the erect attitude. With power on, however, a serious reduction in both longitudinal and directional stability occurred in inverted flight. The effective dihedral was reversed in the inverted flight attitude.

## INTRODUCTION

Fighter airplanes at times assume inverted attitudes while performing combat maneuvers. Inverted attacks are sometimes made because such attacks provide a means for a fast break-away from the opponent. Pilots of some fighter airplanes have recently reported encountering violent and uncontrollable maneuvers that apparently were preceded by flight in the inverted attitude.

In order to obtain pertinent data concerning the stability and control characteristics of airplanes in the inverted attitude, tests were made of a typical present-day fighter airplane model in the Langley free-flight tunnel. The results of force, flight, and yaw-trim tests of the model in the erect and in the inverted attitudes are presented herein.

## APPARATUS

### Wind Tunnel

The tests were made in the Langley free-flight tunnel, a complete description of which is given in reference 1. Photographs of the model flying inverted in the test section of the tunnel are given in figures 1 and 2. The force tests were made on the Langley free-flight-tunnel six-component balance. A description of the balance and its operation is given in reference 2. The balance so rotates with the model in yaw that all forces and moments are measured with respect to the stability axes. The stability axes are axes in which the Z-axis is in the plane of symmetry, perpendicular to the relative wind, and directed downward; the X-axis is in the plane of symmetry, perpendicular to the Z-axis, and directed forward; and the Y-axis is perpendicular to the plane of symmetry and directed to the right.

A stand mounted on the tunnel floor was used for all yaw-trim tests. The model when supported on this stand was restrained in roll, could be locked at any desired angle of pitch, and was completely free to rotate in yaw, except for the negligible ball-bearing friction.

### Model

The $\frac{1}{10}$-scale model used in the tests is representative of present-day fighter design having a wing span of 38.3 feet. The full-scale dimensional characteristics as represented by the test model are given in the following table:

| | |
|---|---|
| Wing span, feet | 38.33 |
| Over-all length, feet | 34.4 |
| Propeller diameter, feet | 11.5 |
| Number of propeller blades | 4 |
| Normal weight, pounds | 6170 |
| Normal center-of-gravity position, percent mean aerodynamic chord | 24.5 |

| | |
|---|---|
| **Wing:** | |
| Area, square feet | 248 |
| Incidence of root (reference) chord, degrees | 1.30 |
| Tip-chord incidence, degrees | -0.45 |
| Aspect ratio | 5.92 |
| Taper ratio | 2:1 |
| Sweepback of leading edge of wing, degrees | 5.12 |
| Dihedral at wing leading-edge reference line, degrees | 5.5 |
| Mean geometric chord, inches | 77.63 |
| Mean aerodynamic chord, inches | 82.54 |
| Distance of leading edge of mean aerodynamic chord behind leading-edge of root chord, inches | 6.11 |
| Flap chord, percent wing chord | 15.0 |
| **Ailerons:** | |
| Chord, percent wing chord | 15.0 |
| Area behind hinge line, percent wing area | 6.6 |
| Span, percent wing semispan | 52.5 |
| Travel, degrees up and down | 15.0 |
| **Horizontal tail surfaces:** | |
| Total area, square feet | 44.1 |
| Span, feet | 13.25 |
| Elevator area behind hinge line, square feet | 10.8 |
| Balance area, square feet | 4.0 |
| Distance from normal center of gravity to elevator hinge line, inches | 206.1 |
| **Vertical tail surface:** | |
| Total area, square feet | 25.48 |
| Rudder area behind hinge line, square feet | 10.05 |
| Balance area, square feet | 1.96 |
| Distance from normal center of gravity to rudder hinge line, inches | 227.2 |

A three-view drawing of the model is given in figure 3 and photographs of the model are shown in figure 4.

Power was supplied to the model propeller by an electric motor rated 1/2 horsepower at 15,000 rpm. The motor was geared to the propeller in the ratio of 3.6:1. All power tests were made with a propeller blade angle of 30° at 0.75 radius.

SYMBOLS

$C_L$ lift coefficient $\left(\frac{\text{Lift}}{qS}\right)$

$C_D$ drag coefficient $\left(\frac{\text{Drag}}{qS}\right)$

$C_m$ pitching-moment coefficient $\left(\frac{\text{Pitching moment}}{qcS}\right)$
(Pitching moment positive when nose moves up.)

$C_l$ rolling-moment coefficient $\left(\frac{\text{Rolling moment}}{qbS}\right)$
(Rolling moment positive when right wing is depressed.)

$C_n$ yawing-moment coefficient $\left(\frac{\text{Yawing moment}}{qbS}\right)$
(Yawing moment positive when nose moves to right.)

$C_Y$ lateral-force coefficient $\left(\frac{\text{Lateral force}}{qS}\right)$

$C_X$ longitudinal-force coefficient $\left(\frac{\text{Longitudinal force}}{qS}\right)$
($C_X = -C_D$ when $\psi = 0$)

$T_c$ effective thrust coefficient $\left(\frac{\text{Effective thrust}}{\rho V^2 D^2}\right)$

$V$ velocity, feet per second

$\rho$ air density, slugs per cubic foot

$D$ propeller diameter, feet

$q$ dynamic pressure, pounds per square foot $\left(\frac{1}{2}\rho V^2\right)$

$c$ mean aerdoynamic chord, feet

$S$ wing area, square feet

$b$ wing span, feet

$\alpha$ angle of attack of thrust line, degrees

$\psi$ angle of yaw, degrees

$\phi$ angle of bank, degrees

$\beta$ angle of sideslip, degrees $(-\psi)$

$C_{l_\beta}$ rate of change of rolling-moment coefficient with angle of sideslip, per degree $\left(\frac{\partial C_l}{\partial \beta}\right)$

$C_{n_\beta}$ rate of change of yawing-moment coefficient with angle of sideslip, per degree $\left(\frac{\partial C_n}{\partial \beta}\right)$

$C_{Y_\beta}$ rate of change of lateral-force coefficient with angle of sideslip, per degree $\left(\frac{\partial C_Y}{\partial \beta}\right)$

$C_{D_\alpha}$ rate of change of drag coefficient with angle of attack, per degree $\left(\frac{\partial C_D}{\partial \alpha}\right)$

$C_{L_\alpha}$ rate of change of lift coefficient with angle of attack, per degree $\left(\frac{\partial C_L}{\partial \alpha}\right)$

$C_{m_\alpha}$ rate of change of pitching-moment coefficient with angle of attack, per degree $\left(\frac{\partial C_m}{\partial \alpha}\right)$

$\frac{-dC_m}{dC_L}$ static margin for power-off condition, chords (x/c)

x distance from center of gravity to neutral point, feet

$\delta_r$ rudder deflection, degrees; positive when left rudder pedal is depressed in erect flight or when right rudder pedal is depressed in inverted flight

$\delta_a$ aileron deflection, degrees

$\delta_e$ elevator deflection, degrees

## TESTS

Tests in which the model simulated a full-scale airplane operating at $T_c = 0$ and 1800 brake horsepower were run at a dynamic pressure of 1.9 pounds per square

foot, which corresponds to an airspeed of approximately 27 miles per hour at standard sea-level conditions and to a test Reynolds number of 166,400 based on the mean aerodynamic chord of 0.646 foot. Tests in which the model simulated a full-scale airplane developing 3100 brake horsepower were run at a dynamic pressure of 1.1 pounds per square foot. The data from all tests are referred to the stability axes in the erect attitude, which intersect at the center-of-gravity location that is 24.5 percent of the mean aerodynamic chord. All tests were made with flaps up.

## Force Tests

Force tests were made to determine the static longitudinal stability of the model operating with power simulating zero thrust and 1800 and 3100 brake horsepower for the full-scale airplane. These tests were made over a range of both negative and positive angles of attack in order to determine the longitudinal stability characteristics in the inverted and erect attitudes.

Values of thrust coefficient required to simulate 1800 and 3100 full-scale brake horsepower over the lift range of the model tests are shown in figure 5. These data are based on an assumed full-scale propeller efficiency of 80 percent.

Force tests over a range of yaw angles from $40^\circ$ to $-40^\circ$ were made to determine the static lateral stability characteristics at angles of attack of $8^\circ$ and $-10^\circ$, which corresponded to lift coefficients of approximately 0.6 and -0.6, respectively. The yaw tests at $\alpha = 8^\circ$ were made with power simulating zero thrust and 3100 brake horsepower for the full-scale airplane and the yaw tests at $\alpha = -10^\circ$ were made with power simulating zero thrust and 1800 and 3100 brake horsepower for the airplane. In all yaw tests, the propeller speed was set to give the proper amount of power at zero yaw and was kept constant over the range of yaw angles.

## Yaw-Trim Tests

The yaw-trim tests were made by deflecting the rudder and noting the resulting trim angle of the model mounted on the stand. Tests of this type are utilized

in the Langley free-flight tunnel to indicate the possible existence of rudder lock. The tests were made for a range of rudder deflections of ±30° for power simulating zero thrust and 1800 brake horsepower for the airplane at angles of attack of 8° and -10°.

## Flight Tests

Flight tests were made to determine the general flight behavior of the model in the erect and in the inverted attitudes over a speed range corresponding to a range of lift coefficients from 0.35 to 0.58. For all flight tests the propeller was removed and the static margin was approximately 0.15.

## RESULTS AND DISCUSSION

### Presentation of Results

In interpreting the results of inverted flight tests, two methods of analysis can be used. The inverted attitude can be considered from the pilot's viewpoint or from considerations of control-fixed stability without regard to the pilot.

The stability and control conditions that would be experienced by the pilot from his inverted position were simulated in the force and yaw-trim tests of the present investigation by testing an erect model at negative angles of attack. The force-test data obtained in this manner are referred to the axes shown in figure 6(b) in order to represent the inverted-attitude condition as it appears to the pilot. In order to determine the control-fixed stability characteristics, however, it was necessary to transfer the force and yaw-trim data to the axes shown in figure 6(c). Figure 6(c) shows that for considerations of control-fixed stability, the change to inverted attitude corresponds to a change in basic configuration. The low-wing design becomes a high-wing design with negative geometric dihedral and the location of the tail surfaces is changed.

A comparison of figure 6(b) with figure 6(c) shows that in order to refer force-test data obtained at negative angles of attack to the axes system of figure 6(c)

the signs of the angles $\alpha$ and $\beta$ and of the coefficients $C_L$, $C_m$, $C_Y$, and $C_n$ must be reversed. The signs of the coefficients $C_D$ and $C_l$, however, do not change for any system of axes. From these considerations, the derivatives $C_{n_\beta}$, $C_{Y_\beta}$, $C_{m_\alpha}$, $C_{L_\alpha}$, and $-dC_m/dC_L$, obtained from negative angle-of-attack data, do not change sign but the sign of the derivatives $C_{l_\beta}$ and $C_{D_\alpha}$ is reversed when they are referred to the axes system of figure 6(c).

All force-test data obtained in the present investigation are presented as the pilot would visualize them. (See fig. 6(a) for axes system in erect flight and fig. 6(b) for axes system in inverted flight.) Some of the force-test data have also been corrected for sign in accordance with the preceding paragraph and are referred to the stability axes (figs. 6(a) and 6(c)). All yaw-trim-test data are also referred to the axes of figures 6(a) and 6(c).

## Longitudinal Stability

The results of force tests made to determine the longitudinal stability of the model are presented in figure 7 using the axes of figures 6(a) and 6(b). These data are shown referred to the stability axes for normal flight (see figs. 6(a) and 6(c)) in figures 8 and 9.

The data of figure 8 show that for zero thrust inverting the flight attitude resulted in an increase in the static longitudinal stability but for power on inverting the flight attitude resulted in longitudinal instability.

The data of figure 8 are rearranged in figure 9 to afford a direct comparison of the zero-thrust and the high-power conditions for the model in the erect and in the inverted attitudes. In the erect attitude, power slightly increased the longitudinal stability, but in the inverted attitude, power was destabilizing and resulted in longitudinal instability. The increase in longitudinal stability with power is attributed in part to the fact that the center of gravity is below the thrust line in the erect attitude and above the thrust line in the inverted attitude. The stabilizing effect of power in the erect attitude is unusual but has been noted in other tests of this design.

The results of the flight tests made with propeller removed indicated satisfactory longitudinal stability characteristics of the model in the inverted attitude. No unusual dynamic stability characteristics were noted in these tests and the flight behavior was similar to that obtained in the flights of the model in the normal erect attitude.

## Lateral Stability

The basic data obtained from force tests made to determine the static lateral stability characteristics of the model are presented in figure 10 for the erect attitude and in figure 11 for the inverted attitude.

Directional stability and trim.- The static directional-stability data for the model in the inverted attitude (fig. 11) have been referred to the stability axes and are compared with corresponding data for the model in the erect attitude in figure 12 to illustrate the effect of attitude upon the static directional stability and trim.

The results presented in figure 12 show that inverting the attitude with zero thrust slightly increased the directional stability for small angles of yaw but reduced the range of yaw angles for which the model was directionally stable. With power on, however, inverting the attitude decreased the directional stability in addition to reducing the range of yaw angles over which the model was directionally stable. The data also show that inversion almost wholly eliminated the favorable effect of power upon the directional stability.

The data presented in figure 12 have been rearranged in figure 13 to show the effect of power in the erect and in the inverted attitude. In the erect attitude, power greatly increased the directional stability at the trim condition ($C_n = 0$) but reduced the range of yaw angles for which the model was directionally stable. In the inverted attitude, power did not substantially affect the directional stability at trim but caused a large reduction in range of yaw angles for which the model was stable.

The difference in power effects between the erect and the inverted attitudes is attributed to the change of

slipstream position with attitude. The results of calculations made by the method of reference 3 to determine the vertical position of the slipstream with respect to the horizontal tail (fig. 14) indicate that for the particular design tested, inverting attitude shifted the high-velocity slipstream jet away from the vertical tail surfaces and that consequently the directional stability contributed by those surfaces was reduced.

The results shown in figure 13 also indicate that the shift of trim point in the inverted attitude with power is in the opposite direction from that in the erect attitude. This shift is attributed to the sidewash angles at the tail induced by propeller rotation. In the erect attitude the vertical tail is located in the upper part of the slipstream jet where rotational effects are such as to cause trim changes (yawing moments) in a negative direction. Inverting the model attitude, however, shifts the relationship of the vertical tail to the slipstream jet so that the vertical tail is partly in the lower part of the slipstream jet and consequently the trim changes are reversed.

The results of the yaw-trim tests, which supplement the force-test results concerning the directional trim characteristics of the model, are presented in figures 15 and 16. The data are plotted in figure 15 to show the effect of model attitude for each power condition and the same data are rearranged in figure 16 to show the effect of power on the directional trim characteristics for the erect and for the inverted attitudes. These results are in general agreement with the force-test results and show that inverting attitude caused the model to trim at larger yaw angles with a given rudder deflection. For the inverted attitude with zero thrust, the fact that the model trims at large yaw angles with rudder deflections greater than -10° indicates that rudder-force reversal (rudder lock) would probably occur in flight at this condition. With power on, similar indications of rudder lock are evident for both the erect and inverted attitudes, and the data indicate that rudder lock is more likely to occur in the inverted attitude. For the inverted attitude with power on the model would trim at normal angles of yaw only with rudder deflections between 0° and 5°.

Dihedral effect.- A comparison of the effective-dihedral characteristics of the model as measured by $C_{l_\beta}$ (slope of curve of rolling-moment coefficient against yaw

angle) was obtained from the data of figures 10 and 11 for the erect and for the inverted attitudes and is shown plotted against the directional-stability parameter $C_{n_\beta}$ in figure 17. The data for the inverted attitude shown in this figure represent the data of figure 11 corrected for sign to the proper system of axes.

The data of figure 17 show that inverting the model attitude for zero thrust reduced the effective-dihedral parameter $C_{l_\beta}$ from -0.0011 to 0.0004, which corresponds approximately to a 7.5° reduction in the effective dihedral. This reduction of effective dihedral with inversion of model attitude is attributed to the change in geometric characteristics accompanying inversion. The test model in the erect position is a low-wing model with 5.5° geometric dihedral, but when inverted it becomes in effect a high-wing model with -5.5° geometric dihedral and therefore has 11° less geometric dihedral. The difference in the change in geometric and effective dihedral is attributed to the fact that, because of wing-fuselage interference effects, a high-wing airplane has a higher effective dihedral than a low-wing airplane with the same geometric dihedral.

Although for control-fixed stability the effective dihedral is negative in the inverted attitude, it might appear positive to the pilot. A comparison of the data of figures 10 and 11 indicates that no change in the sign of the effective dihedral occurs when erect and inverted flight data are referred to the axes of figures 6(a) and 6(b). The pilot should therefore get the same rolling response from rudder kicks in the erect and inverted attitudes and thus might not recognize the existence of the negative-dihedral condition.

The results presented in figure 17 show that power application changed the effective dihedral in the negative direction regardless of model attitude. Consequently, the negative dihedral of the model in the inverted condition became even more negative with power application.

In the flight tests of the model in the inverted attitude with propeller removed, the negative dihedral effect was evidenced by an increase in the difficulty in controlling the model laterally. In order to keep the model flying in the center of the tunnel, the pilot had to use aileron control more frequently than in flights in the erect attitude (positive-dihedral condition).

## CONCLUSIONS

From tests of a model of a conventional low-wing fighter airplane in the Langley free-flight tunnel the following conclusions were drawn regarding the stability and control characteristics of the model in the inverted flight attitude:

1. The flight characteristics of the model in inverted flight with propeller removed were generally satisfactory. The lateral stability characteristics were not so good as those in erect flight, however, because inverting flight attitude changed the effective dihedral from positive to negative. The negative effective dihedral made laterally level flight difficult to maintain.

2. Power application changed the effective dihedral in a negative direction regardless of flight attitude.

3. The effect of power on longitudinal and directional stability was much more serious in inverted flight attitudes than in erect attitudes.

Langley Memorial Aeronautical Laboratory
National Advisory Committee for Aeronautics
Langley Field, Va.

## REFERENCES

1. Shortal, Joseph A., and Osterhout, Clayton J.: Preliminary Stability and Control Tests in the NACA Free-Flight Wind Tunnel and Correlation with Full-Scale Flight Tests. NACA TN No. 810, 1941.

2. Shortal, Joseph A., and Draper, John W.: Free-Flight-Tunnel Investigation of the Effect of the Fuselage Length and the Aspect Ratio and Size of the Vertical Tail on Lateral Stability and Control. NACA ARR No. 3D17, 1943.

3. Goett, Harry J., and Pass, H. R.: Effect of Propeller Operation on the Pitching Moments of Single-Engine Monoplanes. NACA ACR, May 1941. (Classification changed to Restricted Nov. 1944.)

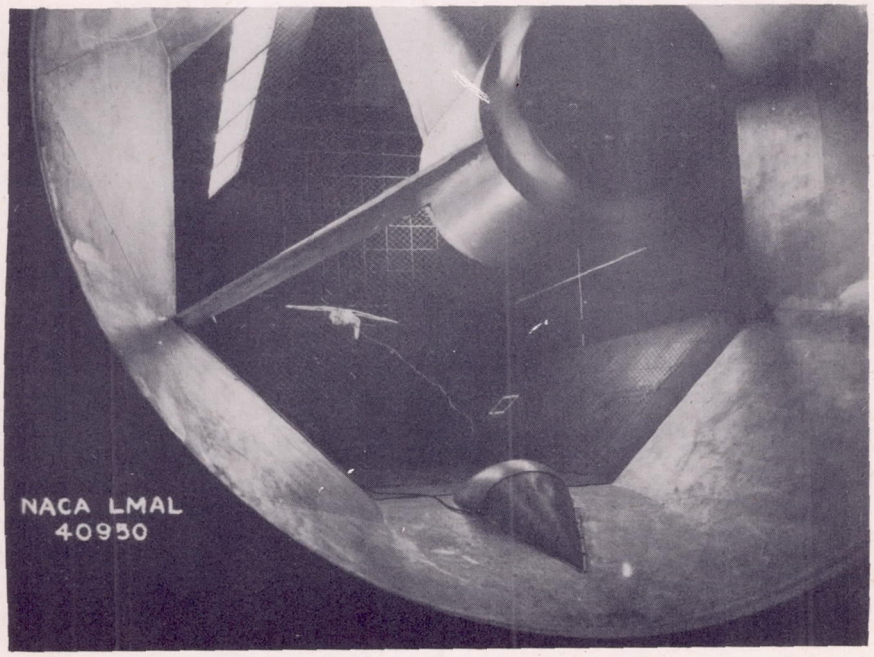


Figure 1.- Test section of Langley free-flight tunnel showing model flying in inverted attitude.

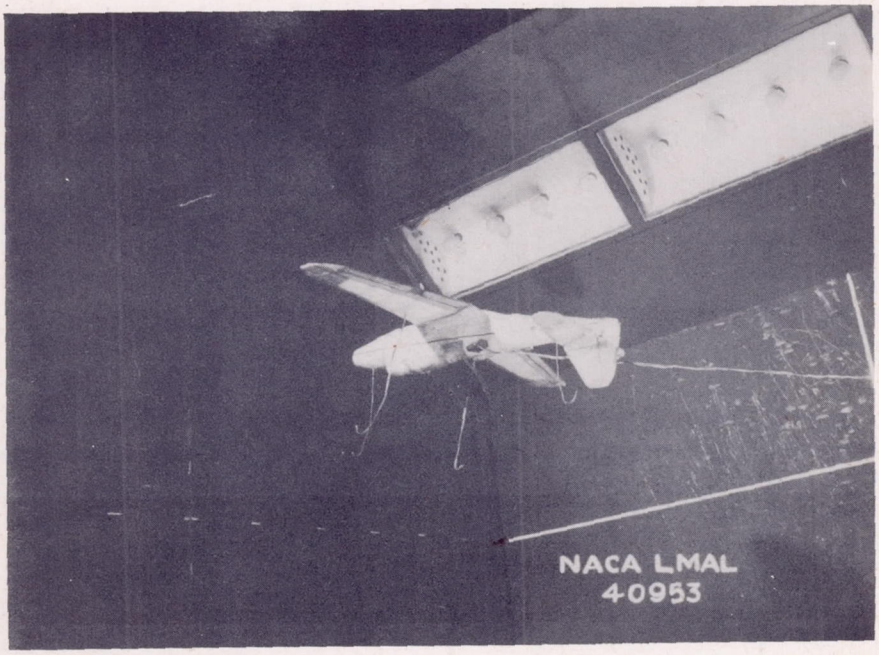


Figure 2.- Model flying inverted in test section of Langley free-flight tunnel.

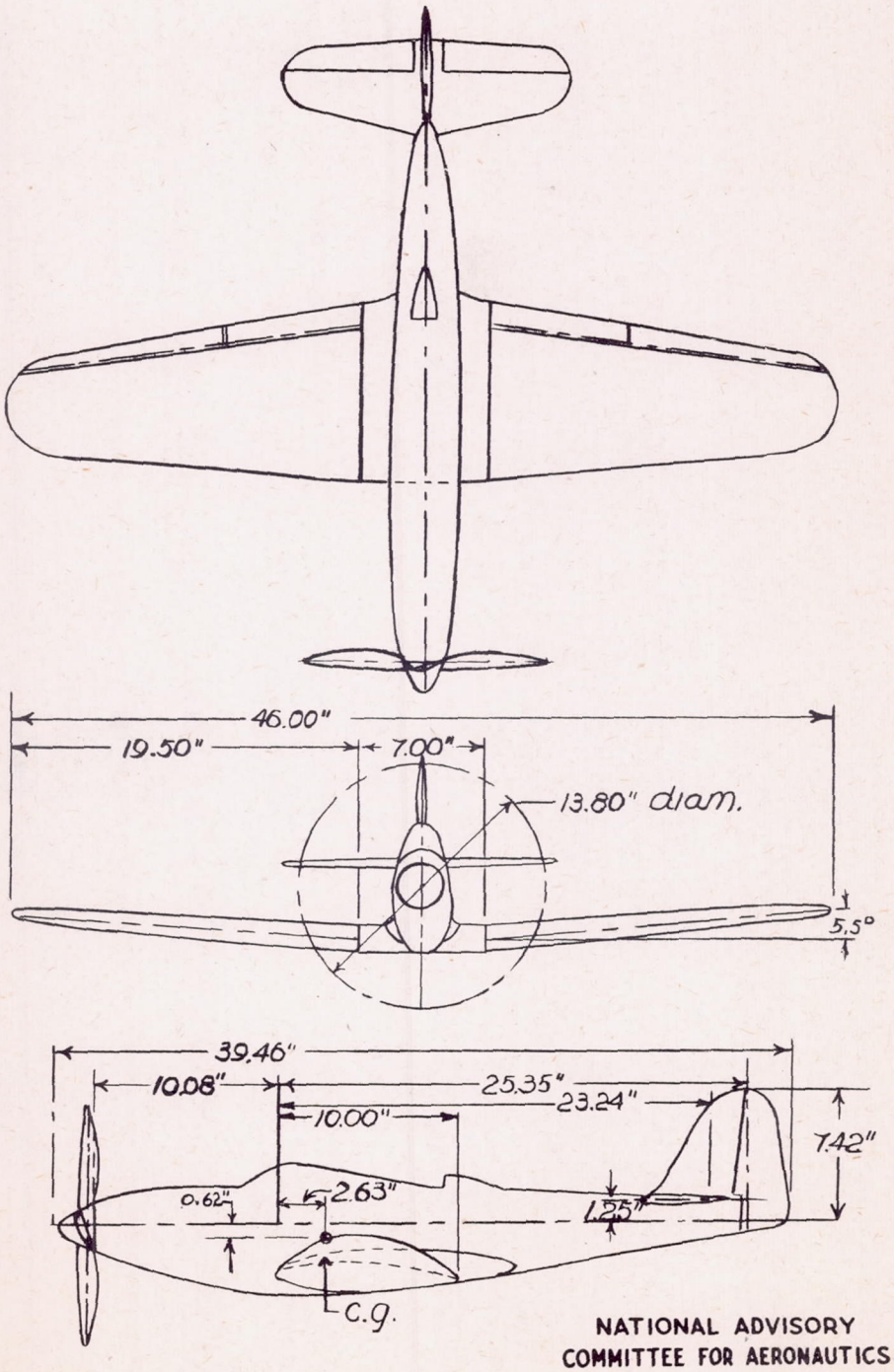


Figure 3.- Model used in free-flight - tunnel investigation of stability characteristics in inverted flight.

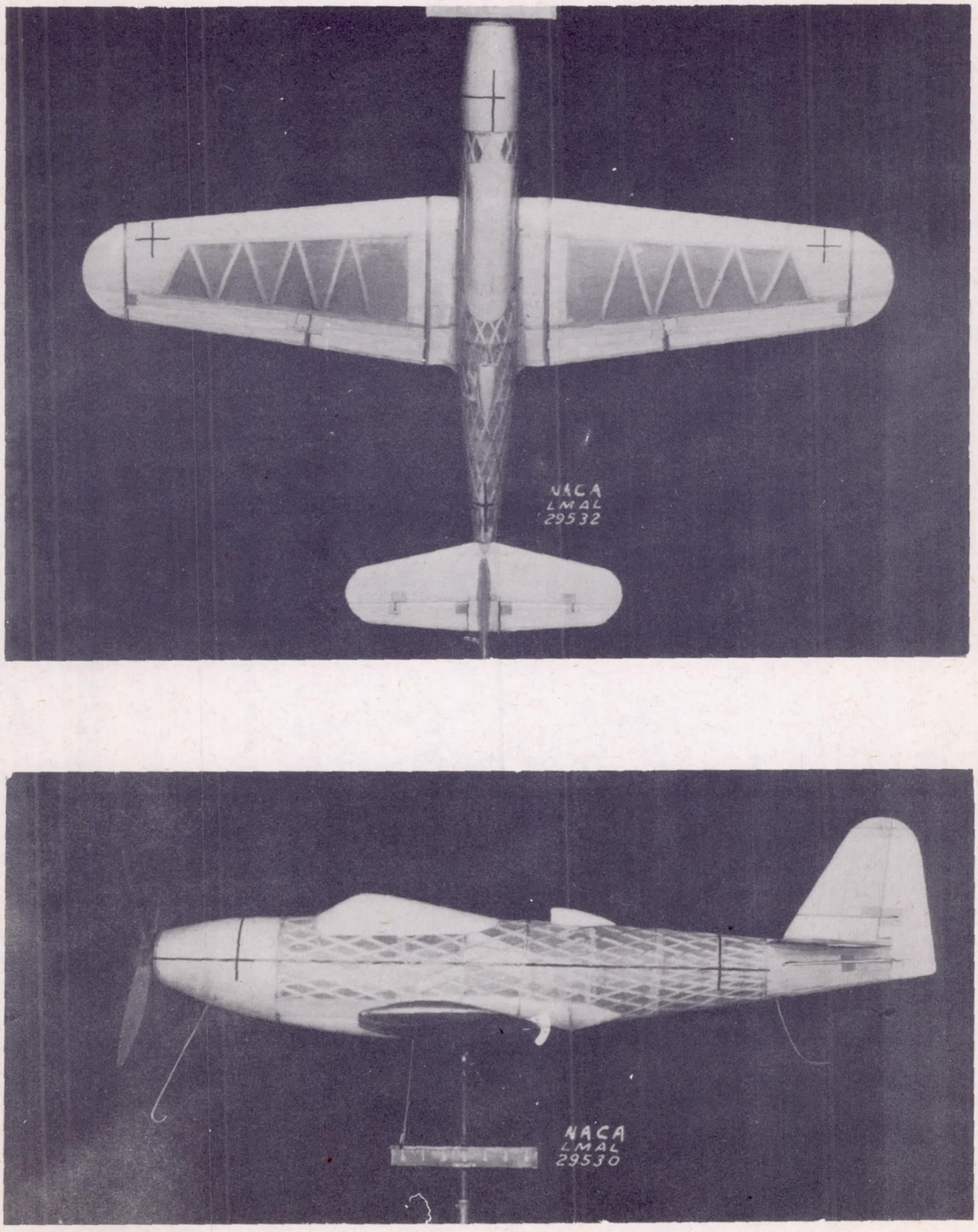


Figure 4.- Plan view and side elevation of model used in inverted-flight investigation in Langley free-flight tunnel.

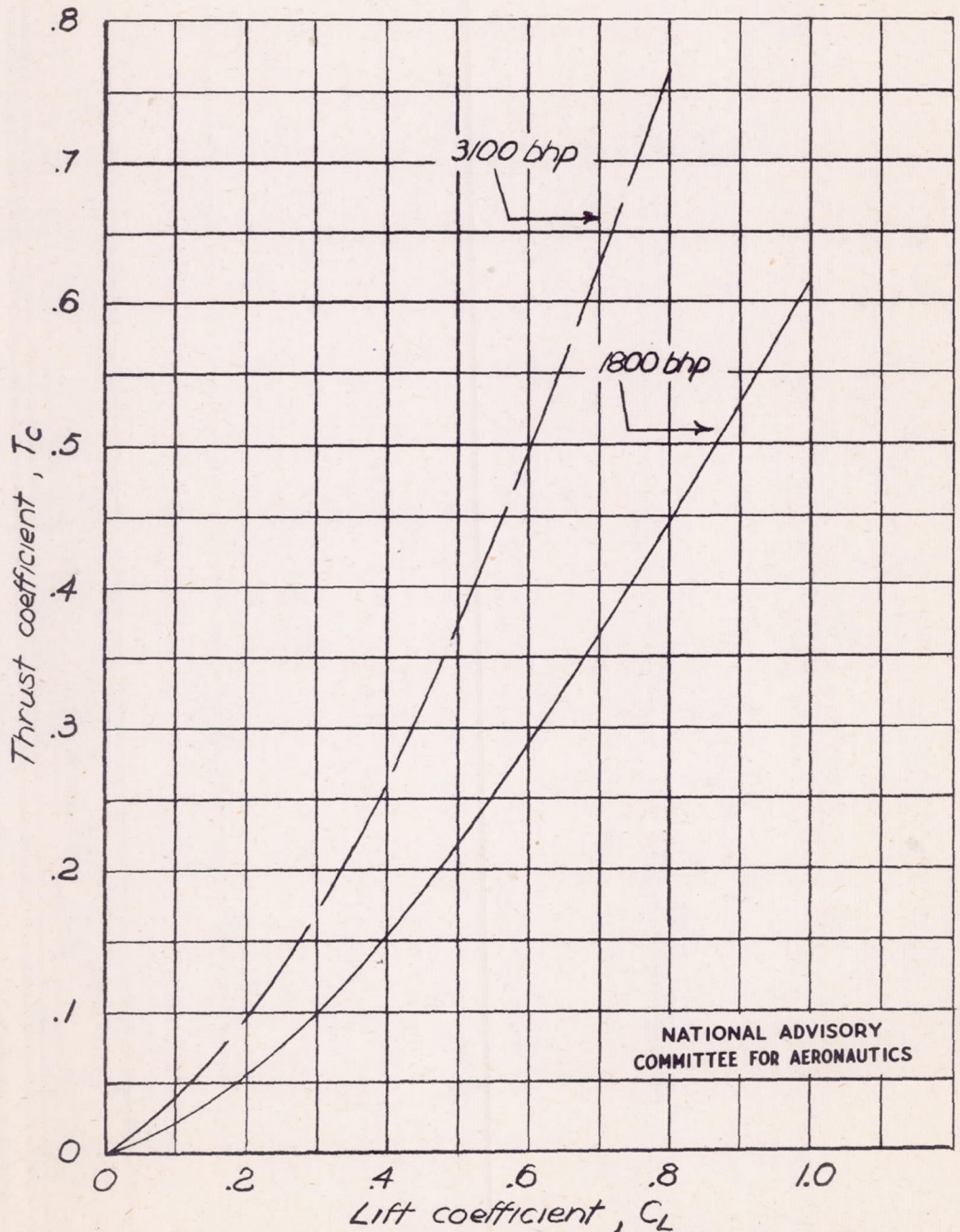


Figure 5.- Variation of thrust coefficient with lift coefficient for test model simulating 1800 and 3100 full-scale brake horsepower at sea level. Propeller efficiency, 80 percent.

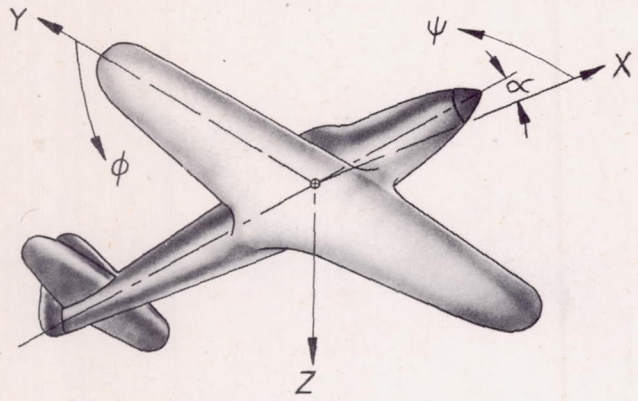


(a) Conventional stability axes for normal erect flight. (Axes about which basic force-test data are measured.)

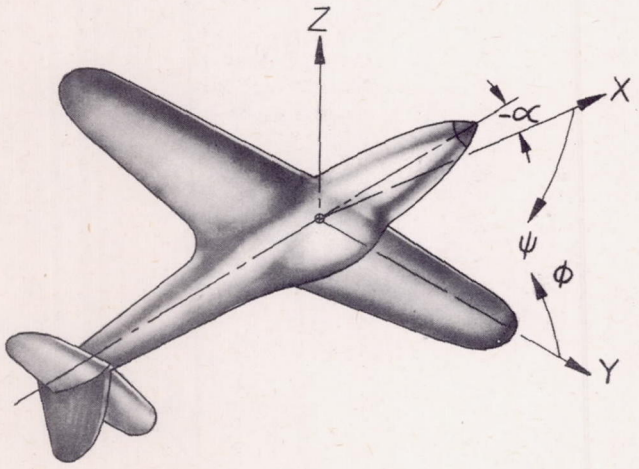


(b) Inverted axes as visualized by pilot in inverted flight. (Axes about which basic force-test data for negative angles of attack are measured.)

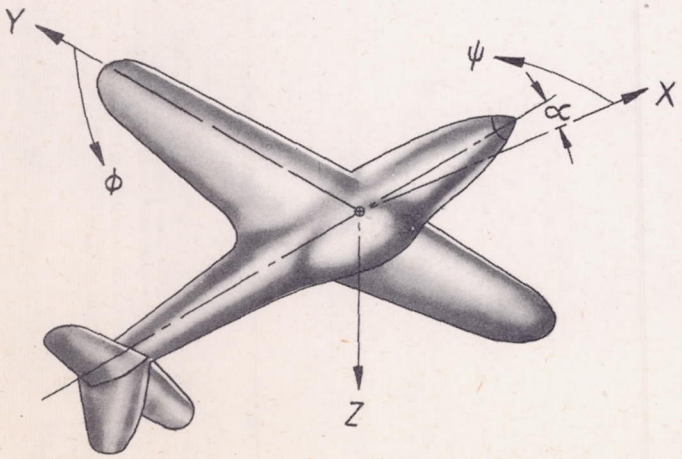


(c) Conventional stability axes for inverted flight. (Axes to which force-test data for negative angles of attack are referred for comparison with data for positive angles of attack.)

NATIONAL ADVISORY
COMMITTEE FOR AERONAUTICS

*Figure 6.- Axes used to evaluate stability characteristics in inverted flight investigation.*

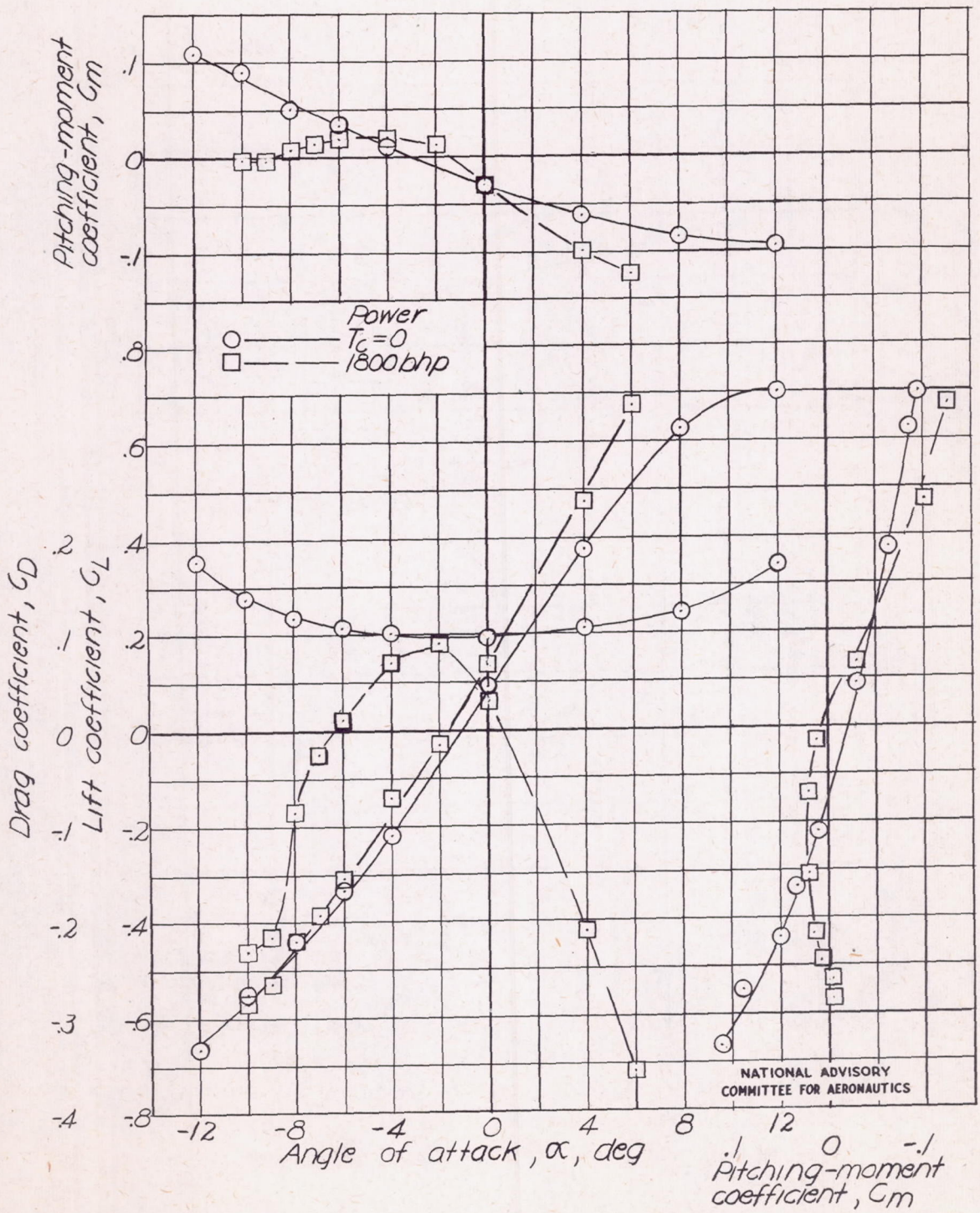


Figure 7.- Variation of aerodynamic characteristics and static longitudinal stability with angle of attack for the test model as obtained from force tests. $\delta_a = \delta_e = \delta_r = 0°$; $\psi = 0°$; $q = 1.9$ pounds per square foot. Data referred to axes of figures 6(a) and 6(b).

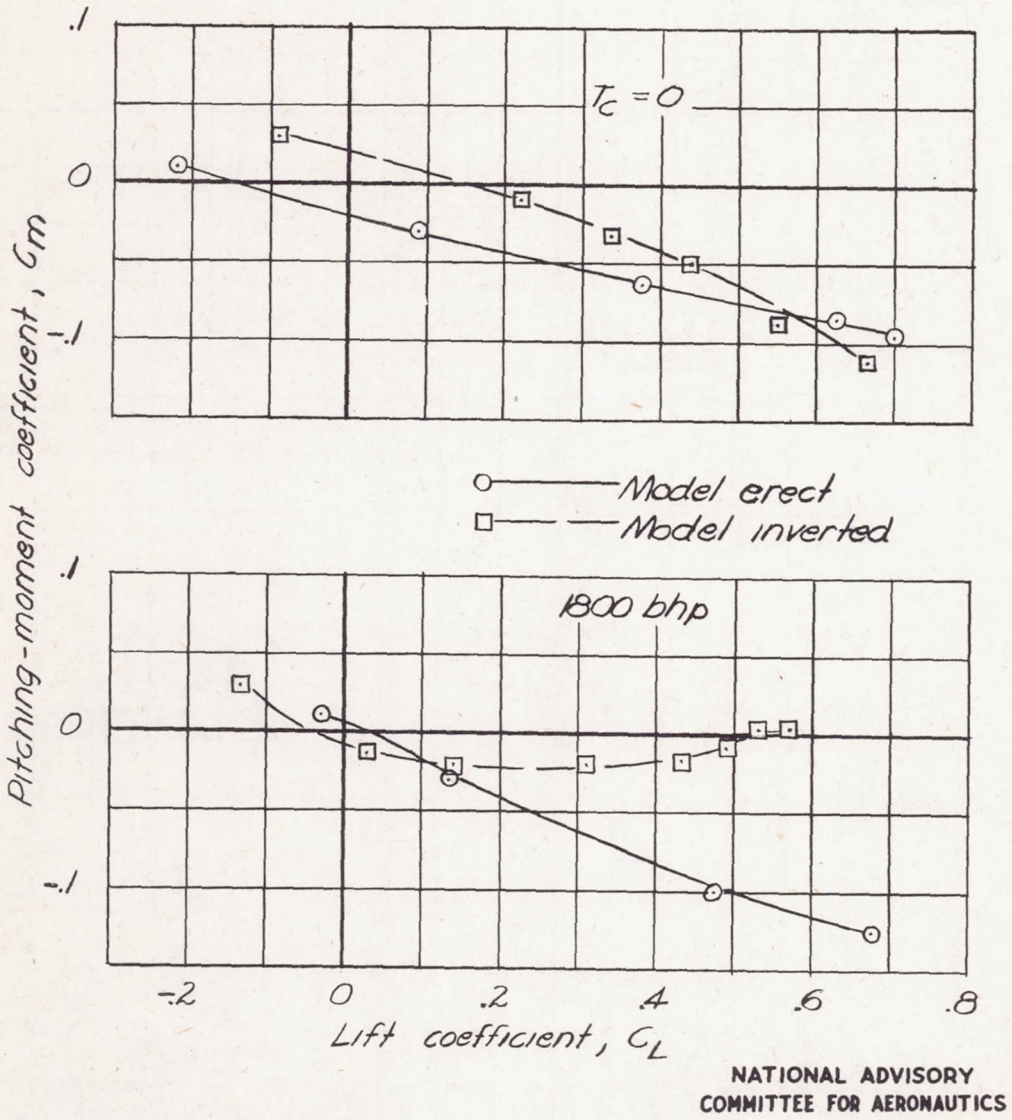


Figure 8.- Effect of attitude on the longitudinal stability characteristics of test model. Data from figure 7 referred to stability axes for normal flight. (See figs. 6(a) and 6(c).) $\delta_a = \delta_e = \delta_r = 0°$; $\psi = 0°$; $q = 1.9$ pounds per square foot.

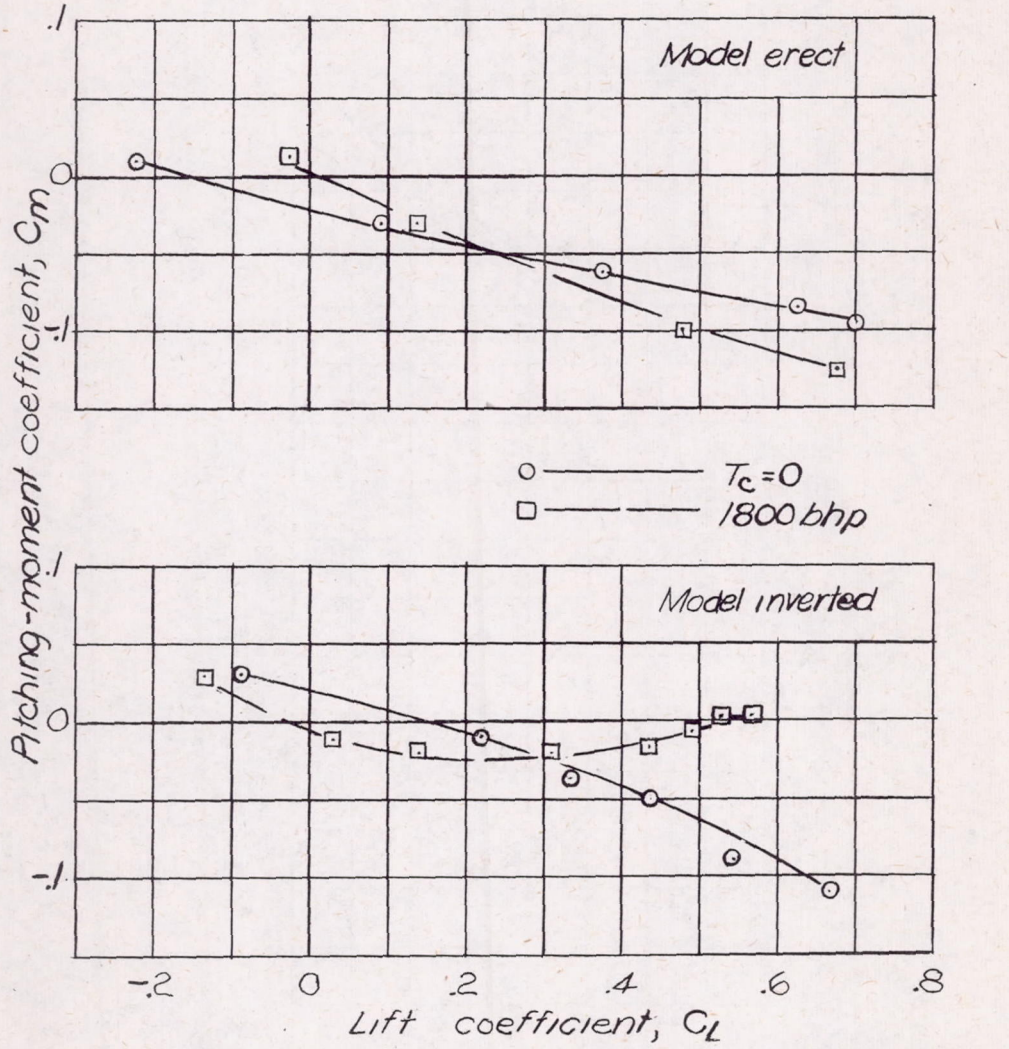


Figure 9. - Effect of power on the longitudinal stability characteristics of test model. Data converted to the conventional stability axes in normal flight. Data taken from figure 7. $\delta_a = \delta_e = \delta_r = 0°$; $\psi = 0°$; $q = 1.9$ pounds per square foot. Data referred to axes of figures 6(a) and 6(c).

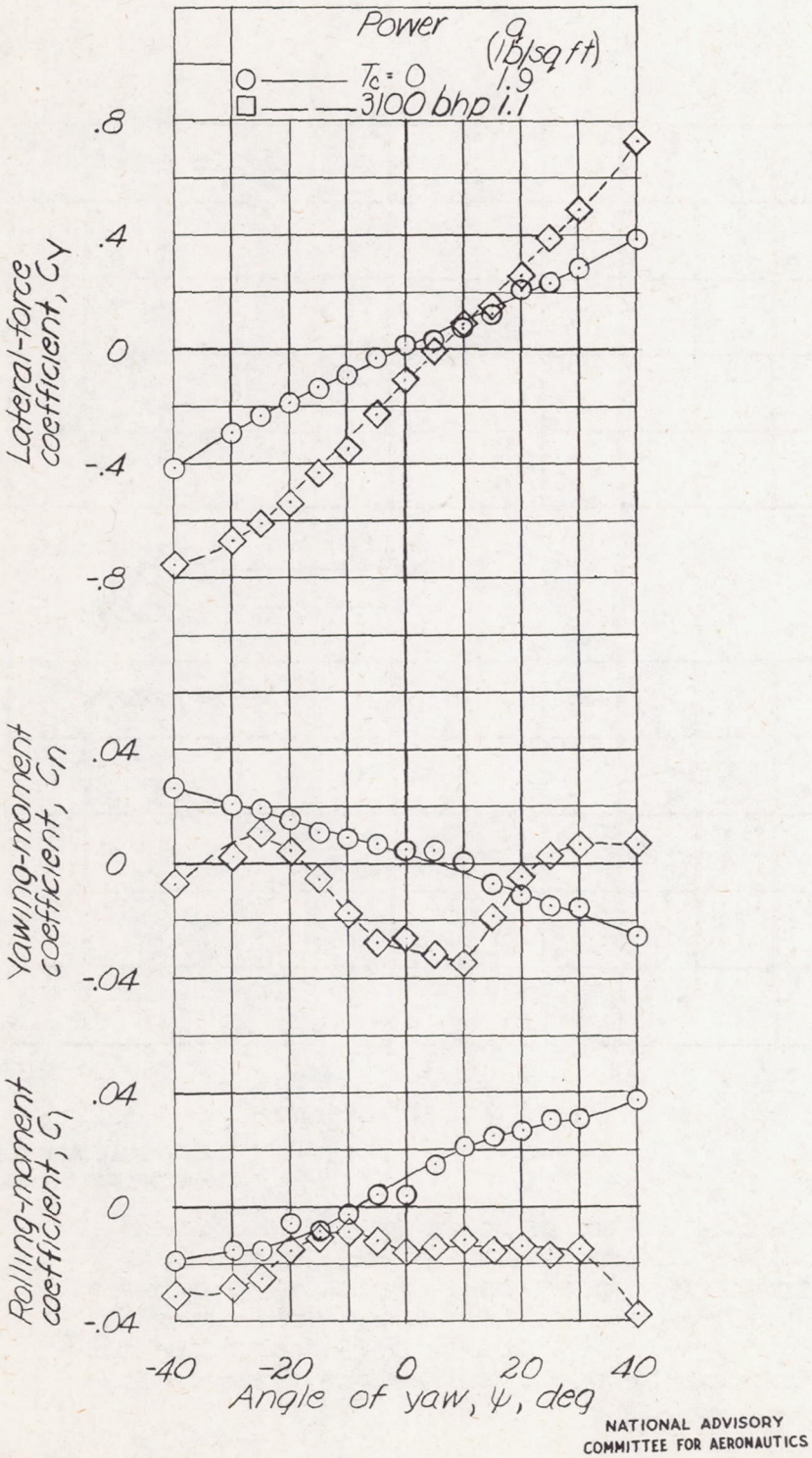


Figure 10.- Effect of power on the lateral stability characteristics in yaw of test model in the erect attitude. $\alpha = 8°$; $C_L = 0.6$; $\delta_a = \delta_e = \delta_r = 0°$. Data referred to axis of figure 6(a).

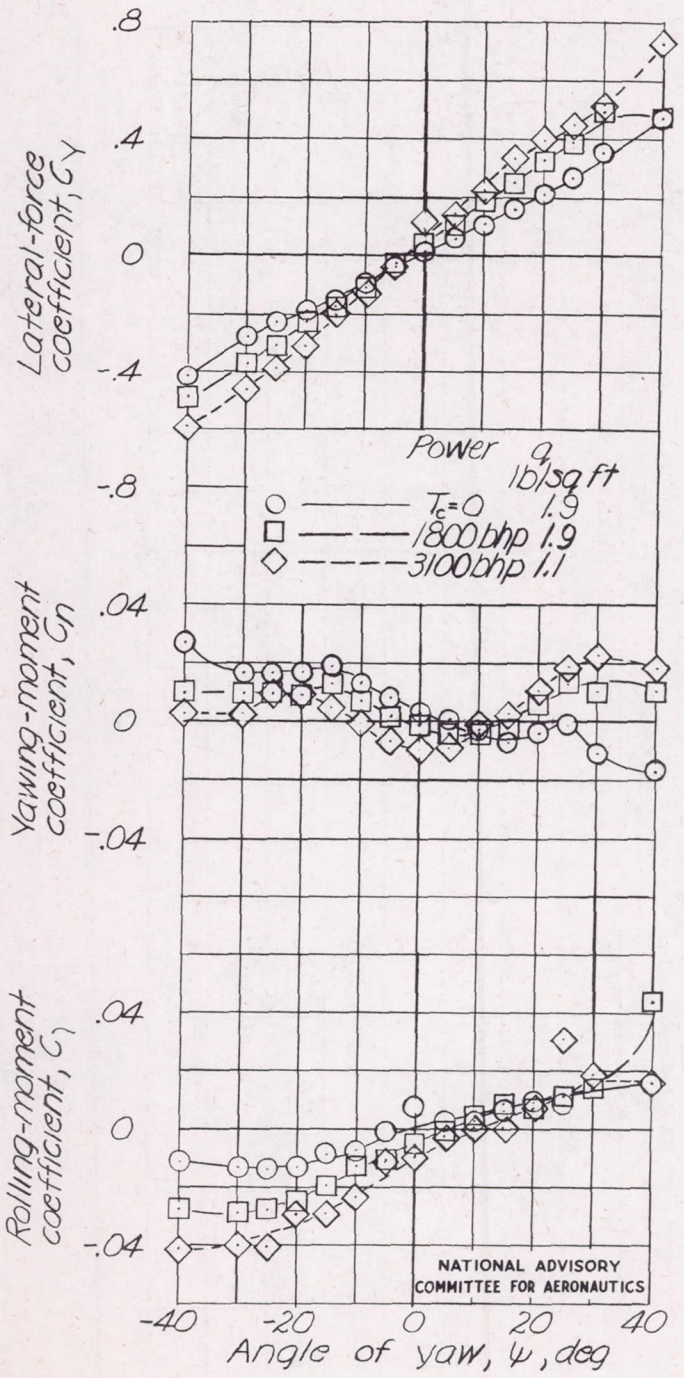


Figure 11.- Effect of power on the lateral stability characteristics in yaw of model in the inverted attitude. $\alpha = -10°$; $C_L = -0.6$; $\delta_a = \delta_e = \delta_r = 0°$. Data referred to axes of figure 6(b).

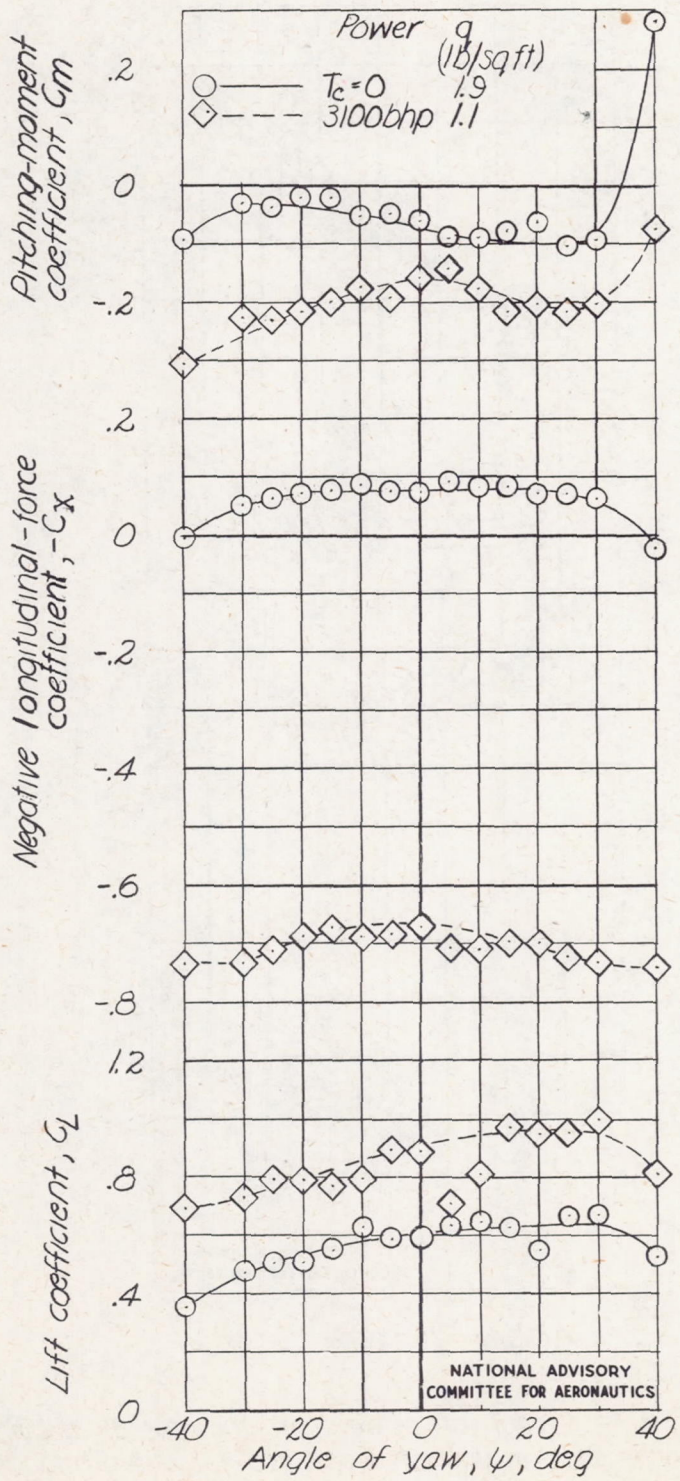


Figure 10- Concluded.

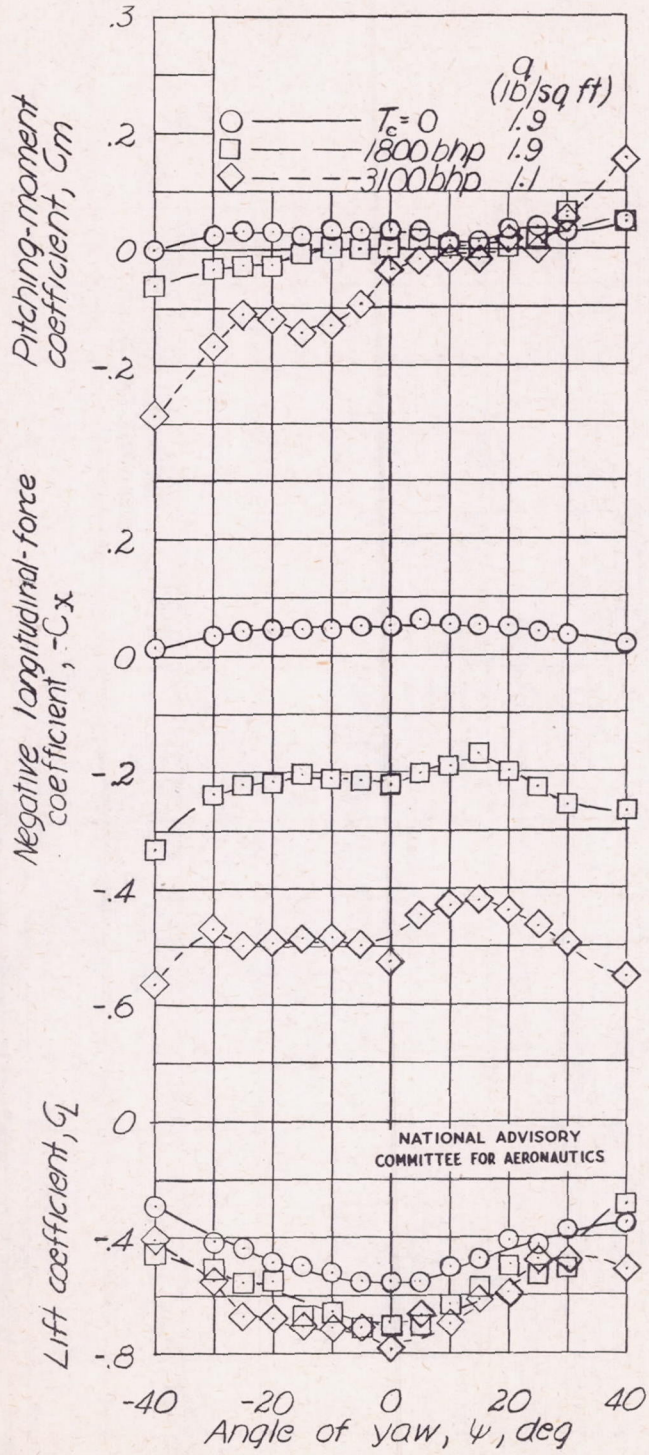


Figure 11.- Concluded.

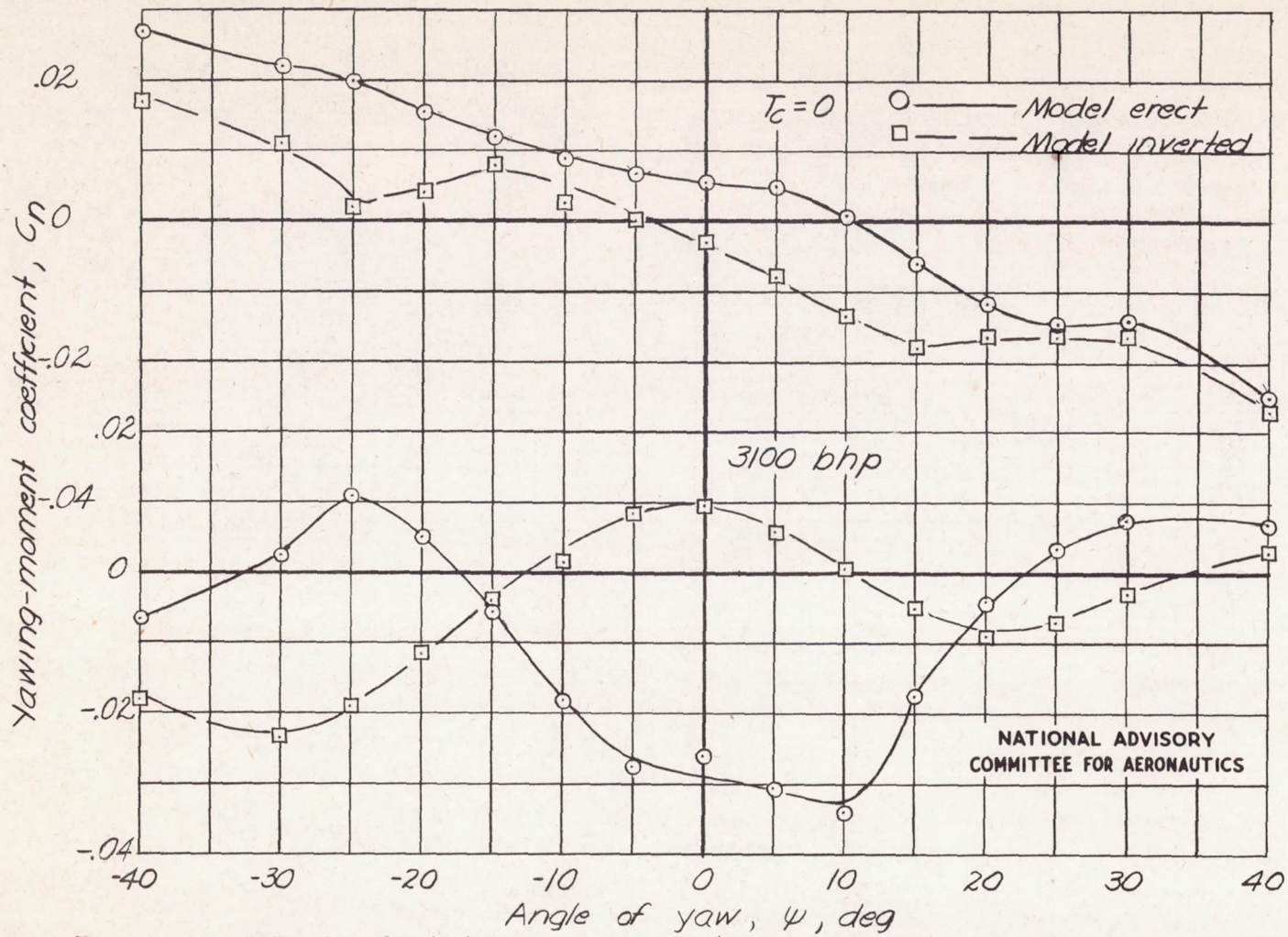


Figure 12.- Effect of attitude on directional stability characteristics of test model for zero thrust and high power. Data from figures 10 and 11 referred to axes of figures 6(a) and 6(c). $C_L = 0.6$; $\delta_a = \delta_e = \delta_r = 0°$.

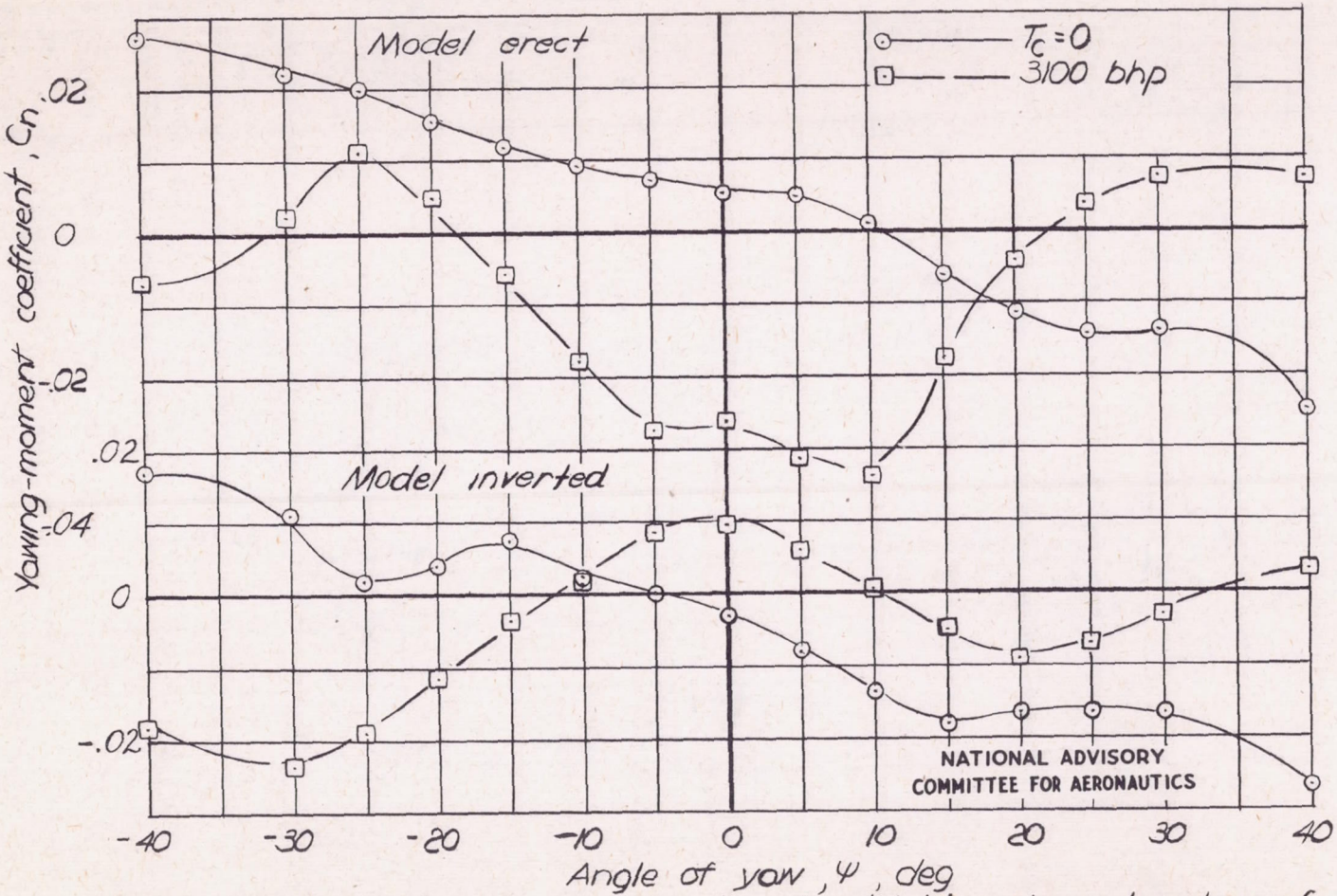


Figure 13.–Effect of power on directional stability characteristics of test model for erect and inverted flight attitudes. Data from figures 10 and 11 referred to axes of figures 6(a) and 6(c). $C_L = 0.6$; $\delta_a = \delta_e = \delta_r = 0°$.

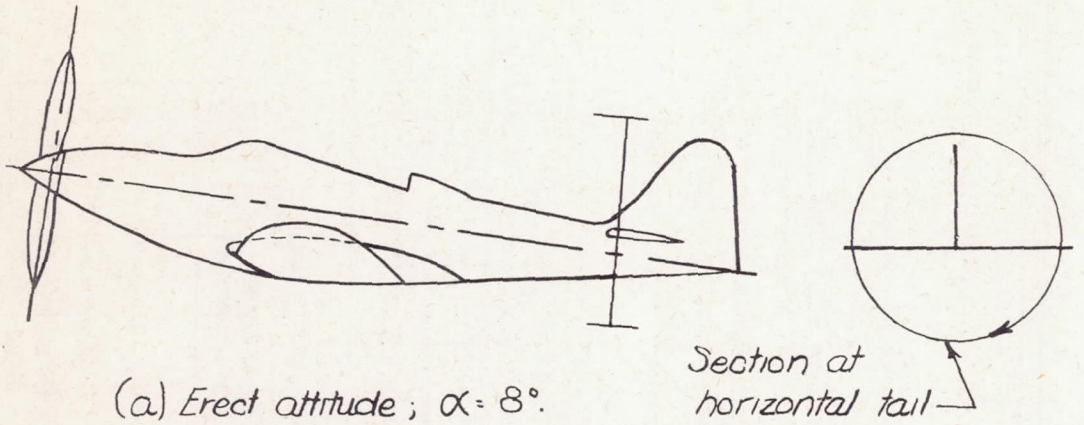


(a) Erect attitude; $\alpha = 8°$.

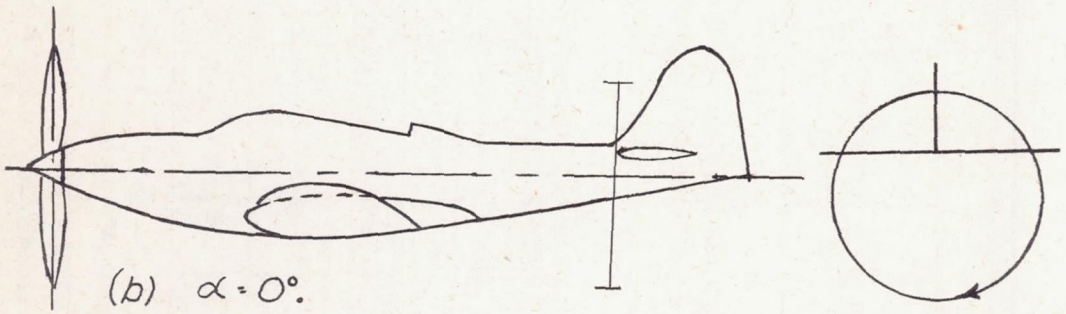

(b) $\alpha = 0°$.

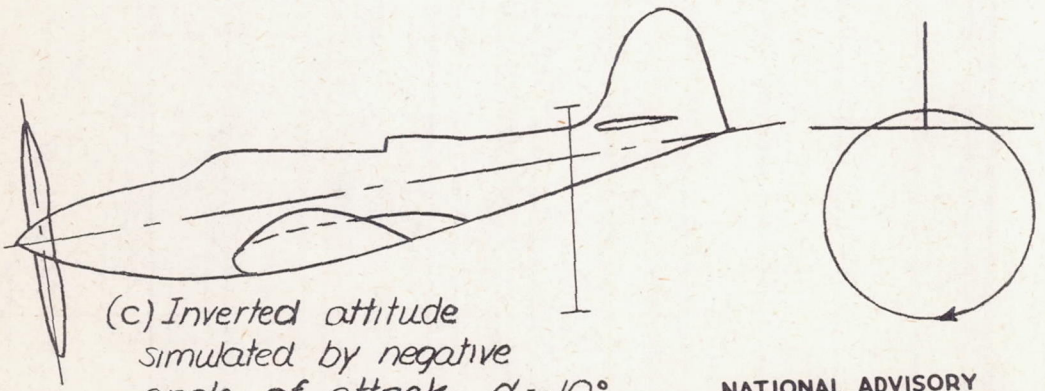

(c) Inverted attitude simulated by negative angle of attack; $\alpha = -10°$.

NATIONAL ADVISORY
COMMITTEE FOR AERONAUTICS

Figure 14.- Vertical position of propeller slipstream calculated for test model in erect and inverted flight attitudes. $\Psi = 0$; 1800 brake horsepower.

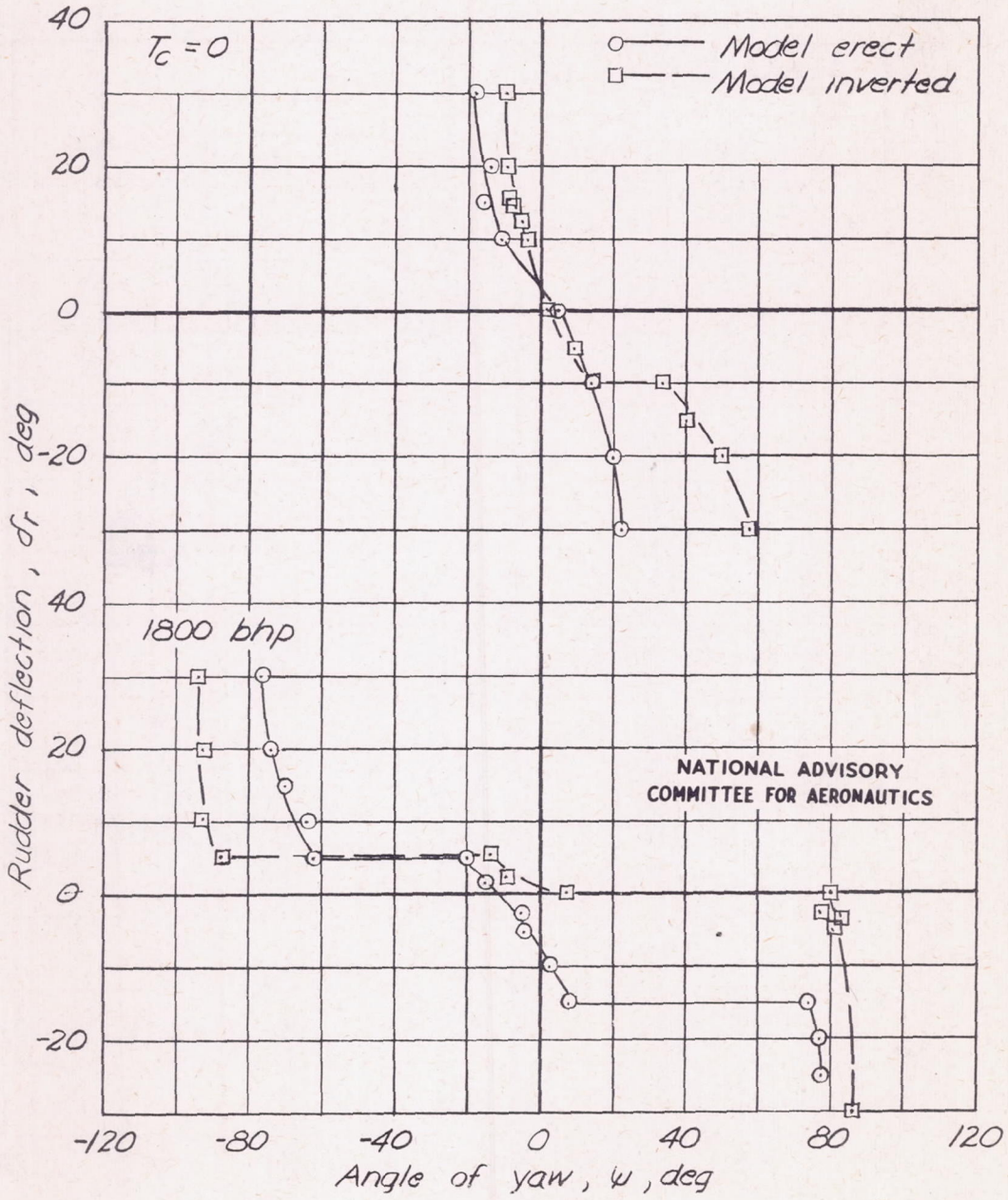


Figure 15.- Effect of attitude on directional trim characteristics of test model used for inverted-flight investigation. Data from yaw-trim tests referred to axes of figures 6(a) and 6(c). $\delta_a = \delta_e = 0°$; $q = 1.9$ pounds per square foot.

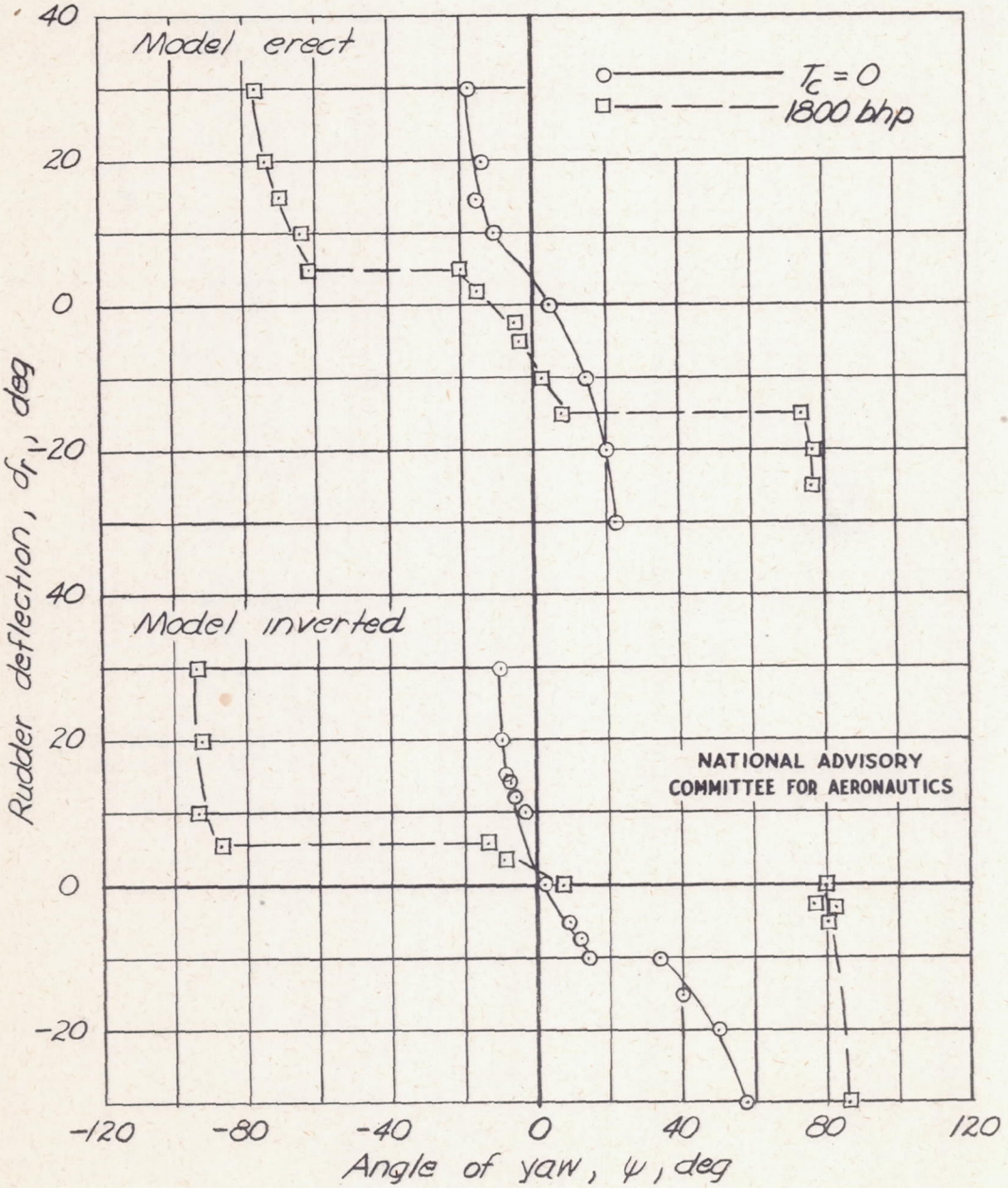


Figure 16.- Effect of power on directional trim characteristics of test model used for inverted-flight investigation. Data from yaw-trim tests referred to axes of figures 6(a) and 6(c). $\delta_a = \delta_e = 0°$; $q = 1.9$ pounds per square foot.

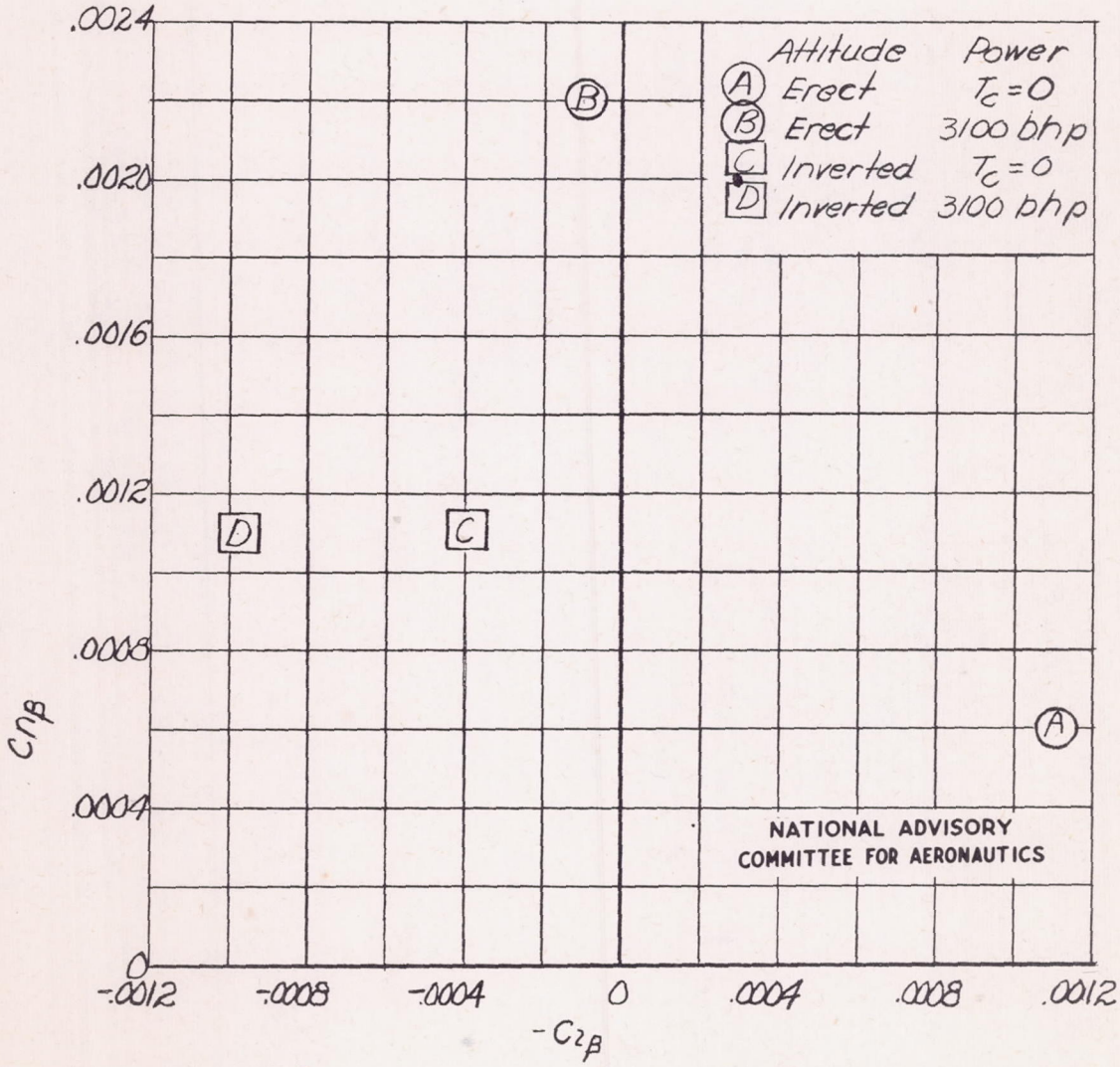


Figure 17.- Variation of effective-dihedral parameter $C_{l_\beta}$ and directional-stability parameter $C_{n_\beta}$ for model attitudes and powers as used for inverted-flight investigation. Data referred to axes of figures 6(a) and 6(c).